Structure, Vol. 13, 703–712, May, 2005, ©2005 Elsevier Ltd All rights reserved. DOI 10.1016/j.str.2005.02.014

A Coiled-Coil Structure of the αIIbβ3 Integrin Transmembrane and Cytoplasmic Domains in Its Resting State

Kay-Eberhard Gottschalk[1,2,*]
[1]Department of Biological Chemistry
The Weizmann Institute of Science
Herzl St. 1
76100 Rehovot
Israel

Summary

One of the hallmark features of the integrin receptors is the ability to transmit signals bidirectionally through the cell membrane. The transmembrane integrin domains are pivotal to the signaling events. An understanding of the signaling mechanism requires structural information. Here, we report a structural model of the transmembrane and part of the cytosolic domains of the αIIbβ3 integrin in its resting state. The model was obtained computationally by a restrained conformational search of helix-helix interactions. It agrees with one published NMR structure of the cytoplasmic complex and can put many experimental findings on structural grounds. According to our model, integrins form an intricately designed coiled-coil structure in the resting state. The conserved Glycophorin A (GpA)-like sequence motif of the α, but not the β, subunit, is in the interface of this model. Based on our calculations and other data, a signaling mechanism that involves a transient GpA-like structure is proposed.

Introduction

Integrins are cellular receptors that are involved in many fundamental cellular tasks. They have been implicated with diverse processes like cell proliferation, migration, cell invasion, and others (Martin et al., 2002). All of these tasks are crucial for multicellular life. On top of their physiological importance, integrins are involved in many pathophysiological processes ranging from tumor metastasis to infertility (Humphries, 2000; Kumar, 2003). To fulfill their diverse tasks, integrins adopt different activation states.

In the ground state, integrins have a low affinity to their extracellular matrix ligands. To increase the affinity, integrins receive intracellular signals. Following inside-out signaling, affinity increase, and subsequent extracellular ligand binding, an outside-in signal is transduced (Kim et al., 2003). This second signal triggers an intracellular cascade.

The importance of the transmembrane (TM) domains for these processes has only been recently realized. The first direct evidence for transmembrane interactions was from electron microscopy images of full integrins that clearly showed electron densities corresponding to the integrin TM domains (Adair and Yeager, 2002). Studies in biological and biochemical test systems, along with crosslinking studies, have further underlined the complex transmembrane association behavior of integrins (Hughes et al., 1996; Kim et al., 2003; Li et al., 2001, 2003, 2004a, 2004b, 2005; Luo et al., 2004; Schneider and Engelman, 2004).

Springer and coworkers elegantly demonstrated that the transmembrane domains separate after the integrins bind ligands (Kim et al., 2003). Afterwards, studying the low-affinity conformation of whole integrins in membranes, they performed crosslinking studies of the TM domains, which provided important structural restraints (Luo et al., 2004). The TM-crosslinked integrins were still able to bind ligands with high affinity after the addition of Mg^{2+} to the extracellular domains. This finding indicates that no conformational change of the TM domains is necessary for a high-affinity integrin conformation. Activating intracellular, membrane-proximal mutations gave rise to nonspecific crosslinking patterns.

For a molecular understanding of integrin signaling and a comprehensive interpretation of the different biochemical data available, a structure of the transmembrane and cytosolic domains is critical. While structures of the extracellular domains of integrins exist (Xiao et al., 2004; Xiong et al., 2001, 2002), the structural models of the transmembrane and cytosolic parts remain ambiguous. Since structures of transmembrane domains are difficult to obtain by classical experimental procedures like NMR or X-ray crystallography, computational modeling has proven to be an excellent tool for the generation of structural models of TM domains, provided that structurally interpretable data are available (Adams et al., 1996, 1998; Fleming and Engelman, 2001; Forrest et al., 1998; Gottschalk et al., 2002; Gottschalk and Kessler, 2004a; Sansom et al., 1997).

Different computational models of the TM domains and three different conformations of the intracellular domains, based on NMR studies of truncated peptides lacking the transmembrane domains, have been proposed (Adair and Yeager, 2002; Gottschalk et al., 2002; Gottschalk and Kessler, 2004a, 2004b; Li et al., 2004b, 2005; Luo et al., 2004; Vinogradova et al., 2002; Weljie et al., 2002).

This paper reports a structural model of the integrin αIIbβ3 transmembrane and part of the cytosolic domains based on computational modeling in combination with reported experimental crosslinking restraints. It will be proposed that integrins can form an intricately designed right-handed coiled-coil structure, and that the low-affinity TM conformation of integrins is not GpA-like. The model is in agreement with many experimental data, including one of the three NMR structures of the cytosolic domains and independent mutational data, which have not been used in the model generation. According to our calculations, the cytoplasmic domains are important for locking the integrin in this non-GpA-like conformation, and our finding is in line with experimental findings (Lu et al., 2001). This result is

*Correspondence: kay.gottschalk@physik.uni-muenchen.de
[2]Present Address: Department of Applied Physics, Ludwig-Maximilians University, Amalienstr. 54, 80799 Munich, Germany.

Table 1. Characterization of Cluster Properties

Helical Cluster	1	2	6	9
Structural parameters				
Energy	–30.7	–30.4	–38.3	–33.9
Crossing angle	14.7	17.3	–11.4	–18.3
Interface area	258.2	259.1	289.6	253.6
Members in cluster	25	21	42	15
Distances				
W968-V696	5	4.8	5	5
V969-V696	5	5	5	5
V971-L697	5	5	5	5
G972-L697	6	7.1	4.4	3.75
G972-V700	4.5	5.1	4.4	4.2
Rmsd to cluster				
1	0	1.03	3.57	4.51
2		0	4.15	5.01
6			0	1.35
9				0
Rmsd to singly restrained runs				
Restrained residues: G972-L697	1.43	1.09	1.24	1.66
Restrained residues: G972-V700	1.76	1.47	0.98	1.37
Restrained residues: V969-V696	0.85	0.92	1.11	1.54
Restrained residues: V971-L697	1.61	2.5	1.53	2.34
Restrained residues: W968-V696	1.93	1.68	0.53	2.61
Average rmsd	1.52	1.53	1.08	1.90

brought into context with the data by Schneider and Engelman (2004) indicating a GpA-like structure of the TM domains. A signaling mechanism with a transient GpA-like structure resolves the apparent contradiction between our model and the data of Schneider and Engelman. The high amount of structural data backing this current model renders it a reliable tool for understanding integrin activation at the atomic level.

Results and Discussion

Restrained Global Conformational Search of the TM Domains

Luo and coworkers performed crosslinking experiments on the transmembrane domains of whole integrins in intact cells (Luo et al., 2004). In their experiments, Luo et al. mutated αIIb and β3 at 10 and 12, respectively, different positions along the transmembrane segment. They tested a total of 120 pairs of cysteine mutants for their ability to form disulphide bridges under conditions that ensured that the integrin is in its resting state (as described in Luo et al., 2004). A specific pattern of crosslinking efficiency was observed when these resting conditions were kept. Under activating conditions, no specific crosslinking pattern was seen, indicating that the crosslinks refer to a single conformation. The crosslinks chosen here as restraints for a conformational search of the integrin TM domains were based on the crosslinking efficiency derived by following the argument of Springer and coworkers (Luo et al., 2004). The crosslinks with the highest efficiency (more than 80% crosslinks) were G972-L697, G972-V700, V969-V696, V971-L697, and W968-V696. All crosslinking data used for the modeling were gathered under identical conditions so that the crosslinking efficiency is directly comparable. These crosslinks are structurally interpretable and can be used as distance restraints in a restrained global conformational search (as described in the Experimental Procedures) (Gottschalk and Kessler, 2004a).

Ten clusters are found by a conformational search with the five restraints. Each cluster represents at least ten highly similar structures with an rmsd of less than 1 Å to at least one other member of the cluster; only four of these clusters have all-helical representative structures (Cluster 1, Cluster 2, Cluster 6, and Cluster 9). The other six representative structures are distorted due to the restraints imposed on the system. Thus, only the four all-helical conformations will be discussed further. Two of the four conformations display a right-handed crossing angle, and two display a left-handed crossing angle (Table 1). The two right-handed helix dimers have a lower energy and tighter packing, as expressed by the distance between the crosslinked residues, than their left-handed counterparts. The two left-handed conformations show slight violations of the distance restraints used during the calculations. The lowest-energy conformation, the right-handed conformation Cluster 6, has the highest interfacial surface area (290 Å), is the representative of the highest populated cluster, and shows the second lowest average distance between the crosslinked residues (Table 1). The right-handed structures and the left-handed structures are very similar (Table 1 and Figure 1). The low rmsd within the two groups is certainly within the error of the method. Certain differences exist between the interfaces of the two groups (Figure 1). While the N-terminal parts, for which the crosslinking restraints exist, have a very similar interface, the interface of the C-terminal parts differs approximately by a 1-residue shift.

A basic problem exists in the context of using different independently obtained crosslinks simultaneously. Crosslinks disturb the energy landscape of the system and can potentially drive it into either nonphysiological conformations or change the equilibrium be-

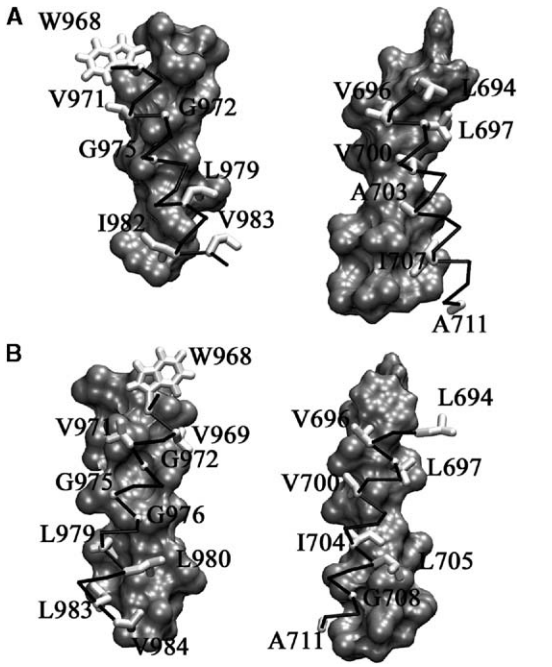

Figure 1. Interface of Cluster 1 and Cluster 6

(A and B) The surface of the interacting partner is depicted in gray, and side chains that are closer than 4.5 Å to the interacting helix are depicted as white sticks. (A) Cluster 1. (B) Cluster 6. Left: The β subunit is shown as a surface representation, and the α subunit is shown as sticks. Right: The α subunit is shown as a surface representation, and the β subunit is shown as sticks.

tween different substates. The crosslinks might refer to different substates; thus, even if all crosslinks can be fulfilled in a single conformation (as shown above), this conformation might not be physiologically relevant, but rather could constitute an unnatural average of substates. To test whether single crosslink restraints—emulating better the actual experiments performed than the simultaneous use of all restraints—drive the system into the same direction as all crosslinks together, five restrained global searches with one restraint each have been performed. The result of these five searches is compared to the previous calculation with all restraints (Table 1). Cluster 6 is well represented by all singly restrained runs. All rmsds are below 2 Å, and two are even below 1 Å, demonstrating that this conformation represents a relaxed state. The other three conformations are less well represented by the singly restrained conformations, indicating that, for those conformations, the restraints put the system under stress. Nevertheless, for all conformations, similar structures are found when using only one restraint or when using all restraints.

The analysis of the calculations shows that: (a) all restraints can be fulfilled in a single helical conformation; (b) similar conformations are found by either using all restraints or only single restraints, indicating that all restraints refer to a single structure; (c) a right-handed conformation, Cluster 6, appears to be favored, since it is the lowest energy conformation that represents the highest populated cluster and is best represented by the singly restrained runs; but that (d) despite the evidence supporting Cluster 6, the crosslinking restraints are not sufficient to unambiguously determine the handedness and the interface of the helix dimer.

Conformational Search of Cytoplasmatically Extended Helices

Since the crosslinking restraints cannot define a single structure of the TM domains, further structural data are needed for an unambiguous model. Based on secondary structure predictions (Gottschalk et al., 2002) as well as NMR data (Vinogradova et al., 2000, 2002, 2004; Weljie et al., 2002) it is known that the membrane-proximal parts of the cytosolic domains are a helical extension of the transmembrane domains. With the knowledge of the secondary structure of this part of the integrin dimer, contact data of the membrane proximal parts of the cytosolic domains can help to further restrain the system. Although three different NMR structures of the complex of the cytosolic domains exist, the lack of a membrane component during structure elucidation and therefore the lack of important environmental restraints might influence the biological significance of the reported structures. For accurate modeling, it is important to use only information on whole integrins in intact cells in order to ascertain biologically relevant data. One restraint that fulfills these criteria is a reported salt bridge between β-D723 and α-R995 (Hughes et al., 1996). Since these two residues are within the helical part of the cytosolic domain, the distance between them can be restrained in a global search of helix-helix interactions with extended helices.

The additional restraint resolves the ambiguity described above. Only one single structural model is found by a restrained global conformational search, if in addition to the crosslinking data, the salt bridge is used as a restraint with extended helices as input. The calculated structure is a right-handed coiled coil. The transmembrane part is very similar to Cluster 6, with an rmsd between the two structures of 1.3 Å.

Following the argument described above, an unrestrained conformational search of the extended helices was performed as a test for the relevance of the restrained search. Failing to find a structure similar to that found for the restrained run would indicate an unreasonable modification of the energy landscape by the restraints. The unrestrained search did not result in a single cluster with the stringent cluster criteria used before (ten structures with a pairwise rmsd of lower than 1.0 Å). Relaxing the cluster criteria to allow an rmsd of less than 1.5 Å resulted in 11 clusters, 5 of which correspond to right-handed structures. One of these five right-handed clusters has a representative structure with an rmsd of 1.4 Å to the cluster from the restrained search. The convergence of the unrestrained search and the restrained search indicates that the restraints can be easily fulfilled without pulling the system into a strained conformation, supporting the notion that the crosslinking restraints and the salt bridge correspond to a single structure. The necessity of relaxing the cluster definitions points to the increased degrees of freedom experienced by the longer helices.

The high amount of structural data used for the gen-

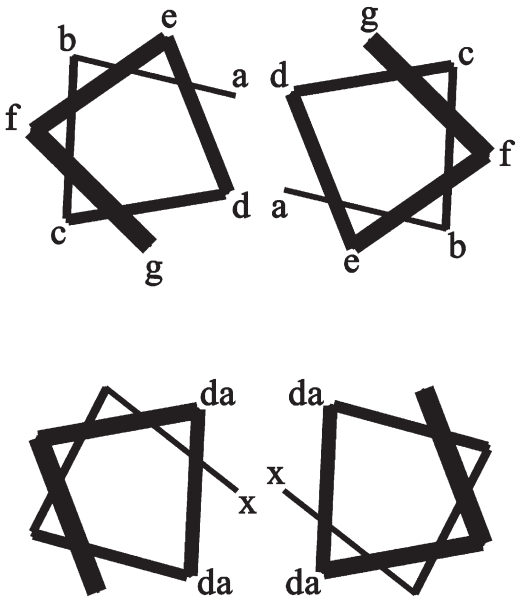

Figure 2. Core Packing in Coiled Coils

Helical wheel representation of coiled coils. In canonical coiled coils, "knobs-into-holes" packing is achieved by distorting the helices to a certain extent. This leads to two periodic core positions, "a" and "d," denoted as a and d layers (top view), in a heptad (a–g) repeat of residues. Insertion of four residues (stutter) causes a rotation of the helices against each other, transforming the original a layers into x layers, and the d and e layers into so-called da layers. X layers are directly facing either each other or da layers, depending on the exact location of the stutter (bottom). The 11/3 periodicity of a right-handed coiled coil can be formally described as a canonical heptad together with a stutter. The existence of x layers disfavors the formation of right-handed coiled-coil dimers.

eration of this model, the fortunate placement of the restraints at each end of the helix, and the convergence of the unrestrained and the restrained searches suggest that the model is of high confidence. The number of intersubunit restraints is of the same order as that encountered for NMR structures of dimeric proteins or peptides (Dehner et al., 2001; Vinogradova et al., 2002; Weljie et al., 2002). Thus, the resolution can be compared to a low-resolution NMR structure, which already allows for a detailed discussion of the structure.

The Coiled-Coil Structure of the Integrin

To better understand the analysis of the integrin coiled-coil structure, a short description of the structural parameters of coiled coils is given here, in line with the excellent description of these structures in (Lupas and Gruber, 2005). Canonical, straight α helices have 3.6 residues per turn (Pauling et al., 1951). As first proposed by Crick (1952), packing of side chains in the core of interacting helices leads to a distortion of the individual helices. The distortion allows regular interactions of side chains every seven residues, or two turns of each helix in a so-called "knobs-into-holes" packing, in which the residues ("knobs") are not directly facing each other but rather are packed into "holes" of the helix partner. This leads to a distorted helix with 3.5 residues per turn. The individual positions in a helix with a heptad repeat are labeled "a"–"g" (Figure 2, top). In soluble proteins, the core residues (a layers and d layers) tend to be more hydrophobic, while the flanking residues tend to be more hydrophilic. The coiled-coil structure thus leads to a heptad repeat of the chemical nature of side chains. Such a coiled-coil structure forms a left-handed supercoil and is found in leucine zipper proteins (Lupas and Gruber, 2005; O'Shea et al., 1991). The periodicity of a helix in a coiled coil distorted in the described way is termed 7/2 (seven residues in two turns). Pauling suggested different regular periodicities for each helix, such as 11/3 (11 residues in 3 turns, 3.67 residues per turn) or 15/4 (3.75 residue per helical turn) (Pauling and Corey, 1953), which have indeed been observed in protein structures (Stetefeld et al., 2000). While the 7/2 periodicity has less residues per turn than the canonical α helix and therefore results in a left-handed coiled-coil, 11/3 or 15/4 periodicities have more residues per turn and lead to right-handed coiled-coils. The 11/3 periodicities can be thought of as a regular heptad repeat with the insertion of four residues, a so-called stutter (Lupas and Gruber, 2005). Stutters affect the core packing of the residues significantly. They can be imagined as a rotation of the individual helix. Residues are shifted from position "a" to the center of the interface core and now occupy a position labeled "x," while residues from positions "d" and "e" are moved to positions labeled "da" (Figure 2, bottom). This transforms the knobs-into-holes packing into a knobs-into-knobs packing for the x layer. x layers may be combined with da layers to avoid clashes, depending on the exact location of the stutter.

How does the calculated integrin structure fit into this picture? The following structural description refers to the result of the constrained search. Judged from the crossing angles, the coiled-coil structure is divided into two parts: the N-terminal part follows an 11/3 periodicity, and the C-terminal part follows a 15/4 periodicity. Both periodicities are found among right-handed coiled coils. The N-terminal part needs to compensate for the existence of x layers, which can potentially lead to clashes. Here, according to the structural model, a strategy is pursued that has also been observed for the right-handed (albeit antiparallel) coiled-coil structure of the Mnt repressor (Nooren et al., 1999). As observed in the Mnt repressor structure, and also in the integrin model described here, x layers are combined with da layers in order to avoid clashes, and small residues are favored. In detail, the interacting residues are as follows: W968 in x position and V696/L697 in da position; G972 in x position and V700/M701 in da position; G975/G976 as da and I704 as x; and only L979-G708 as x-x (Figure 2). The C-terminal part is rather canonical, with L983-L712 in a position, A986/M987-W715/K716 in de positions, V990-I719 in h position, and K994-D723 in l position (Figure 2). The nomenclature of the layers follows the one outlined by Lupas and Gruber (2005). The positions of the 15/4 periodicity are labeled "a" to "o."

If one presumes that all integrins share their basic structure, the small residues in x positions or in da positions close to x positions should be conserved. Indeed, the prevalence of small residues at positions G972 and G976 in α-integrin sequences led to the postulation of a GpA-like structure with a GxxxG motif of α homodimers and α/β heterodimers (Adair and Yeager, 2002;

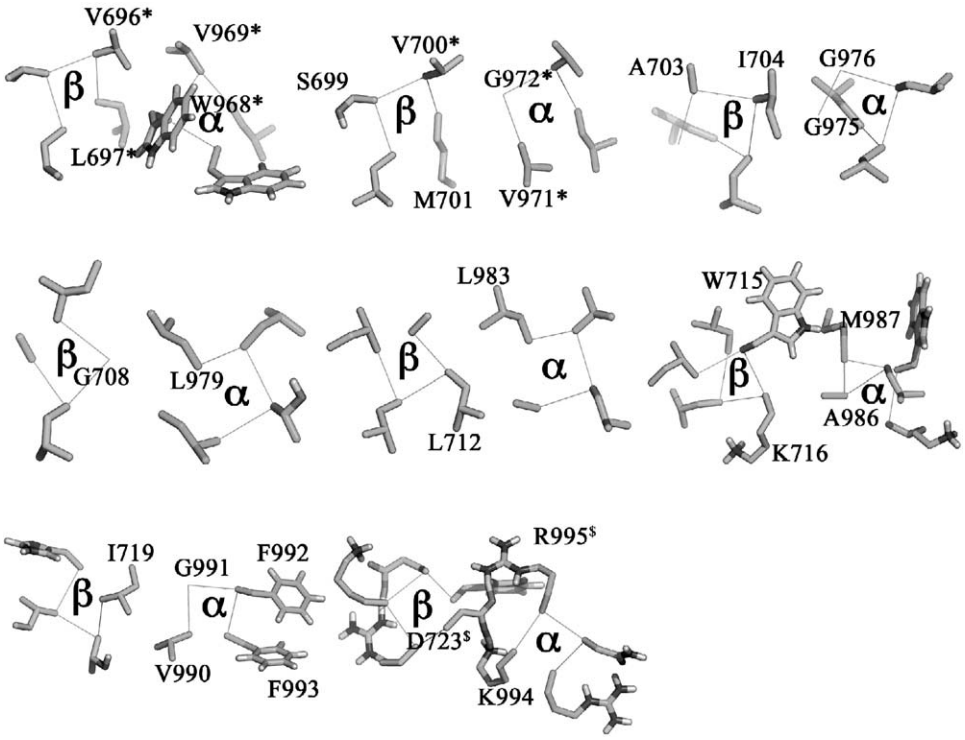

Figure 3. Interacting Residues in the Coiled-Coil Model

Each turn of the helix is shown together with the interacting residues as sticks. Cyan, β subunit; green, α subunit. The crosslinked residues are marked with a star, and the salt bridge used as a restraint is marked with a "$."

Gottschalk et al., 2002; Gottschalk and Kessler, 2004a; Li et al., 2004b; Schneider and Engelman, 2004). Recently, Li et al. (2005) showed that mutations disrupting the G972xxxG976 motif activate integrins. Since integrin activation is accompanied by TM domain separation, Li et al. argued that the most probable explanation for the activation is the disruption of the heteromeric interface. Our structural model reflects this explanation.

G708 has a fundamental role in our model. It is at the only position at which two x layers face each other, and no other side chain is suitable for this fold. Remarkably, G708 is completely conserved in all integrins (with the exception of the unusual β8 integrins) (Gottschalk et al., 2002). Interestingly, a G708N mutation and an M701N mutation have been shown to increase constitutive fibrinogen binding as well as β homotrimerization (Li et al., 2003). Both of these residues are at the heterodimeric binding interface according to our model. Originally, the fibrinogen binding increase has been attributed to the increased tendency of the mutants to form β trimers, implying that these trimers facilitate cluster formation. Our model offers an additional explanation: while the heterodimeric coiled coil can accommodate an M701N mutation (although the exact structural or energetic consequences of such a mutation cannot be accurately described by the model), G708N is disruptive. Therefore, a G708N mutation might have a double effect: it stabilizes the homomeric β-integrin trimer, and, additionally, it destabilizes the heteromeric dimer, as opposed to the M701N mutation. Indeed, the effect of the G708N mutation on fibrinogen binding is twice the effect of the M701N mutation (Li et al., 2003).

Of the highly conserved sequence, G991 FFKR995, G991, K994, and R995 are involved in intersubunit interactions according to our model. D723, which has been shown to form a salt bridge with R995, binds in between K994 and R995, forming the only electrostatically complementary patch on the binding site. F992A and F993A mutations have been shown to activate integrins (Vinogradova et al., 2000). In our model, they are not involved in intersubunit interactions, a fact that raises questions about the possible cause of the observed activation. Different lines of argument can be pursued to resolve the apparent contradiction. Based on NMR studies, these residues have been implicated in structural interactions with the nonhelical tail of αIIb (Vinogradova et al., 2000). Therefore, as suggested before (Gottschalk et al., 2002; Vinogradova et al., 2000), the nonhelical tail of the α subunit might be involved in activity regulation, and the F992A and F993A mutations might alter the tail conformations. Furthermore, recent glycosylation studies indicate that both phenylalanines are located at the membrane/water interface (Armulik et al., 1999; Stefansson et al., 2004). Mutating these residues might therefore disturb the anchoring of the helix in the membrane, leading to an activating conformational change of the complex. Additionally, in the wild-type protein, these residues might destabilize the activated state or stabilize a transition or intermediate state; thus, a mutation can potentially shift the equilibrium toward the activated conformation.

The GpA-like motif of the β subunit (S699xxxA703) is not in the interface of the resting state of integrin αIIbβ3 (Figure 3). This is in contrast to data by Schneider and

Engelman, who demonstrated for integrin $\alpha 4\beta 7$ by using their GALLEX system that the GpA-like motifs of both subunits, in our case G972xxxG976 of αIIb and S699xxxA703 of $\beta 3$, are contributing to the heteromeric dimer formation of integrin TM domains in biological membranes (Schneider and Engelman, 2004). Schneider and Engelman did not find the interactions reported here. Since the system used in their studies is highly dependent on the relative orientation of the TM helices to the DNA binding domain, the construct used might have prevented the formation of the interface described here.

Surprisingly, even the unrestrained search of the extended helices did not find any GpA-like conformation of the TM domain. This seems to be in contrast to our earlier results (Gottschalk et al., 2002), in which we showed that an unrestrained search of only the transmembrane domains favors a GpA-like conformation. In our search protocol, we demand that the helices contact over the entire length. This restraint apparently disfavors a GpA-like TM domain structure, indicating that the cytoplasmic parts of the helices prevent the transmembrane parts from forming their most stable conformation. Thus, the cytoplasmic parts are mandatory for maintaining the integrin in the resting state. This is a well-known fact in integrin research: deleting the cytoplasmic helices or mutating key residues activates integrins (Lu et al., 2001; Luo et al., 2004). Despite the fact that a GpA-like structure is not found in the calculations described here, the fundamental question of whether or not the tendency to form the GpA-like structures found by Schneider and Engelman is an artifact of the construct used or reflects a biologically significant conformation, which might either be transient or reflects some signaling intermediate, remains open and will be discussed in greater detail later.

Comparison with Structural Data

For the cytoplasmic interactions between αIIb and $\beta 3$, three NMR models (1KUZ.pdb, 1KUP.pdb, 1M8O.pdb) have been reported (Vinogradova et al., 2002; Weljie et al., 2002). Since our model includes overlapping fragments with all three models, a direct comparison is possible. While rather large discrepancies exist between our model and 1KUP or 1M8O, the model is in very good agreement with 1KUZ, with a CA rmsd on the order of 2.3 Å. The main difference between our model and 1KUZ is that our model is restrained to obey approximately a canonical α-helical structure, but that due to either lacking restraints or the flexibility of the biochemical construct used during structure determination, 1KUZ shows rather large deviations from helicity. The relative orientation between the two fragments is virtually identical (Figure 4). This shows that the model presented here, based only on restraints obtained from whole integrins in biological membranes and the NMR structure of a short cytosolic fragment of the same complex, converges to a single, consistent model. Since the two structures were obtained independently, by using different sets of restraints obtained by different methods, they mutually strengthen the biological significance of both the present model and the NMR structure 1KUZ.

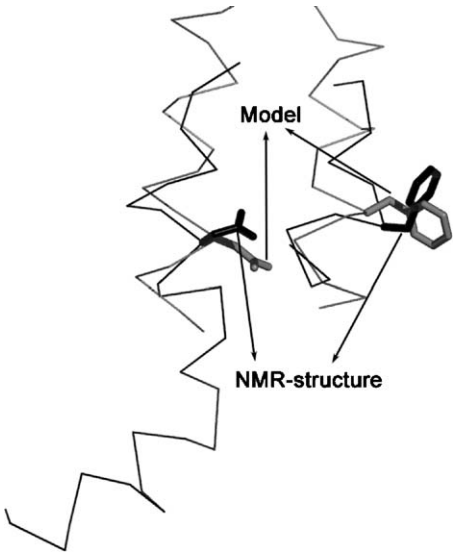

Figure 4. Superpositions of the Coiled-Coil Model with the NMR Structures of the Cytosolic Domains

Superposition of the coiled-coil model (gray) with the NMR structure of the cytoplasmic complex 1KUZ (red). The backbone rmsd is 2.3 Å, and the relative orientation (as exemplified by residues F992 and D723) is identical, but deviations from helicity occur in 1KUZ.

Different models have been proposed for the TM domain conformation in the resting state. Based on their EM images and conservation criteria, Adair and Yeager (2002) proposed a right-handed coiled coil with a GpA-like interface. Our model shows that, in the resting state, the GpA-like sequence of the α subunit, but not the β subunit, is in the interface. Nevertheless, our coiled-coil model fits well into the electron densities of Adair and Yeager (data not shown). Springer and coworkers threaded the sequences on a GpA template and minimized the distance of the crosslinked residues (Luo et al., 2004). Although this procedure reproduces approximately the interface found here, it restricts the crossing angle to an artificially high value, which is difficult to bring into context with the cytoplasmic salt bridge. Furthermore, the rotation angle is restricted so that no adaptation to the sequence can occur. Li et al. (2005) used a Monte Carlo approach to model the resting state with their mutational data as a guideline. This approach led to ambiguous transmembrane models, which differed mainly in the crossing angles, with right-handed crossing angles overrepresented. Their interface is similar to the one reported here. Using an unrestrained global search of helix-helix interactions, we proposed an ambiguous structural model of the TM domains with nearly the identical interface as reported here (Gottschalk et al., 2002). The rmsd of our unrestrained model, obtained without any biochemical data, and our experimentally based model presented here is 2.3 Å, underlining on the one hand the power of the methods used, but stressing on the other hand that for higher resolution models experimental data are mandatory.

One drawback of our prediction scheme is that due

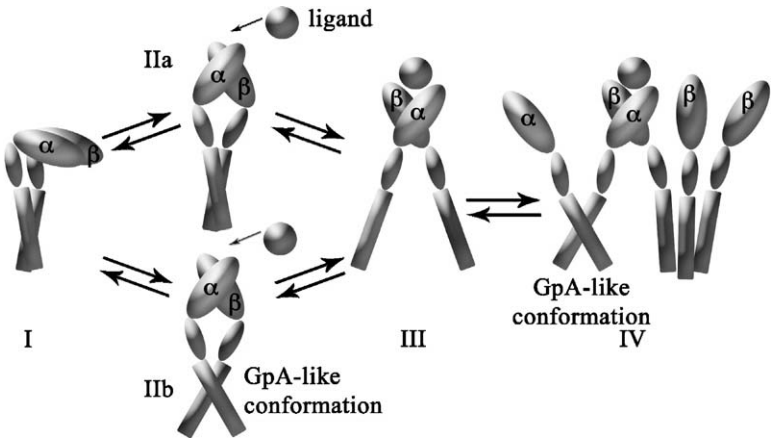

Figure 5. Structural Model of Integrin Activation and Signal Transduction

The resting state (I) can be transformed from the outside to a high-affinity state without change in TM conformation (IIa). Inside-out signaling requires a TM conformational change (IIb). Ligand binding leads to TM separation (III) and possibly to the formation of new coiled coils (IV).

to the restraints applied, significant deviations from helicity, like π bulges, cannot be predicted correctly; however, small deviations necessary for supercoiling are easily compatible with the restraints used. The restriction of the secondary structure to nearly canonical α helices in our model is a possible source of error, which cannot be easily adjusted. Nevertheless, CD and NMR studies, as well as secondary structure prediction, indicate that the part modeled here is predominantly α helical (Gottschalk et al., 2002; Li et al., 2001, 2002; Vinogradova et al., 2000, 2002, 2004; Weljie et al., 2002). Yet, certain deviations from helicity have been observed, possibly affecting the accuracy of our model (Li et al., 2002; Vinogradova et al., 2000, 2002; Weljie et al., 2002). These deviations might well be a consequence of the experimental conditions. The current state of the art does not allow us to include major deviations from helicity into the modeling procedure due to the rapidly increasing degrees of freedom. The ability to include all experimental restraints into a single, consistent α-helical model supports the notion that the modeled part is indeed predominantly α helical.

A Signaling Mechanism

One of the hallmark features of integrins is the bidirectional signaling. Due to a couple of seminal papers by the group of Springer and coworkers, the structural basis for signaling is mainly solved (Kim et al., 2003; Takagi et al., 2001, 2003; Xiao et al., 2004). Binding of signaling molecules induces a structural rearrangement, which separates the integrin stalk regions, and as such the TM and intracellular domains. The details of these steps still remain elusive. It has been shown that locking the transmembrane helices by crosslinking still enables high-affinity binding of extracellular ligands (Luo et al., 2004). Thus, the TM domains can remain associated, even in their resting position, and still the extracellular domains can adopt a high-affinity conformation. Nevertheless, a conformational change of the TM domains has to occur in order to transmit a signal from the inside through the membrane.

Our model shows that the GpA motif of the β subtype is not involved in the TM interactions in the resting state, as opposed to the GpA motif of the α subtype. On the other hand, three points argue for the existence of a GpA-like structure of some heteromeric integrin conformation: (a) a conserved GpA-like sequence motif in nearly all of the α and β subtypes; (b) the results of a global search of TM interactions of 16 integrin subtypes, demonstrating that a GpA-like conformation is the lowest-energy conformation of these helix pairs (Gottschalk et al., 2002); and (c) the GALLEX results by Schneider and Engelman (2004), which underline an intrinsic propensity of integrin TM domains to form a dimer with the GpA motif in both of the helix interfaces. An intriguing possibility to integrate our structural model presented here with the data by Schneider and Engelman is the postulation of a transient GpA-like transmembrane structure after the binding of intracellular ligands. The intracellular ligands can initially disturb the cytoplasmic interactions and thus remove the constraint imposed on the transmembrane domains. These can relax into their most stable state and form a GpA-like structure. This would resolve the apparent contradiction between the GALLEX data and the global conformational search of the TM domains on the one hand, and the model presented here on the other hand. Such a transient transmembrane conformational change from the conformation presented here to a GpA-like conformation can then trigger the extracellular conformational change necessary for raising the affinity.

The TM separation, which in the case of a specific, directed process has to work against the high-viscosity membranous environment, is probably energetically costly. Forming new transmembrane interactions can potentially provide part of the energy necessary. Mutational work by Li et al. (2003, 2004b, 2005) demonstrated that stabilizing β trimers and α dimers activate integrins. Thus, the formation of trimeric coiled coils of the β subunit or dimeric coiled coils of the α subunit might be such an energy-providing step. Yet, according to our model of the αIIbβ3 heterodimer in its resting state presented here, and the model of the β3 homotrimer presented earlier (Gottschalk and Kessler, 2004a), the interaction interfaces of the heterodimer and the homotrimer overlap. In both cases, the helix face of M701 and G708 is buried in the interface. Thus, in order to trimerize, the TM helices have to separate first. A transient GpA-like structure would facilitate the trimeri-

zation and thus also the transmembrane separation, since it would expose the M701-G708 helix face. Such a scenario would indicate that unwinding of the hetero α/β coiled coil with potentially the parallel formation of the trimeric β coiled coil would be the key steps in the transmembrane signaling of integrins. The unwinding of a coiled-coil structure in the course of integrin signaling has recently been proposed as a possible signaling mechanism based on glycosylation mapping results (Stefansson et al., 2004). Yet, the biological relevance of the trimeric β coiled-coil state has to be tested further. The activating effect might be a secondary effect, in which the trimer formation indeed facilitates the transmembrane separation as outlined above, but is not mandatory for signaling.

A similar scenario is conceivable with regard to αIIb. According to our structural models, this should be a less efficient facilitator of TM separation (and thus of integrin activation), since all states, the resting state, the GpA-like state, and the homodimeric state, share the same interface (Gottschalk et al., 2002; Gottschalk and Kessler, 2004a). Therefore, mutations that disrupt the heteromeric interface also disrupt the homodimer. Indeed, such hetero- and homodimer interrupting mutations have been shown to activate integrins, indicating that α homodimers are not necessary for integrin activation (Li et al., 2005). Still, stabilization of the homodimers pulls the conformational equilibria toward the active state, in line with and following the argument by Li et al. (2005).

Summarizing the arguments, an integrin signaling mechanism, which integrates the biochemical data known and is consistent with the structural models generated, involves four states (Figure 5). A resting state (state I) is activated either by intracellular ligands (state IIb; shown with the transient GpA conformation) or by extracellular effectors (state IIa). Binding of intracellular or extracellular ligands separates the transmembrane domains (state III) and might induce homomeric interactions (state IV). As shown by Li and coworkers, disturbing either the resting state or stabilizing the homomeric interactions shifts the equilibrium to the right. The transient heteromeric GpA conformation might facilitate TM separation and homomeric coiled-coil formation.

Coiled coils are protein building blocks with fascinating properties. Changes of their oligomeric state, unwinding, and reforming are widely used cellular mechanisms (Gruber and Lupas, 2003; Martin et al., 2004), most impressively demonstrated by membrane fusion proteins (Bullough et al., 1994; Dormitzer et al., 2004; Weis et al., 1990). As demonstrated here, our structural studies together with biochemical data indicate that this versatile structural tool is also involved in integrin signaling.

Experimental Procedures

All of the calculations have been performed with the molecular modeling and manipulation program CNS, version 1.1 (Brunger et al., 1998). The OPLS united atoms force field parameters with explicit aromatic and polar hydrogens were used (Jorgensen and Tiradorives, 1988). The electrostatic and van der Waals term was cut off at 13 Å for all calculations, employing a shift function starting at 10 Å to ensure a smooth transition of the energy to zero.

The applied method follows closely the protocol used for the successful prediction of the GpA structure as well as for the prediction of phospholamban and the integrin heteromeric and homomeric TM conformations (Adams et al., 1995, 1996; Gottschalk et al., 2002; Gottschalk and Kessler, 2004a). Different dimer conformations were generated with all possible rotation angle combinations ω of 0°–360° in 45° increments, starting with both left- and right-handed crossing angles Ω of 25° and –25°, respectively. Initially, the helices were positioned with a vertical shift of zero. Four trials with different random velocities were carried out starting from each conformation by using simulated annealing of all atomic coordinates, leaving all degrees of freedom free to vary. First, the system simulated 5000 steps with a step size of 0.001 ps at 600 K; second, the system simulated 5000 steps with a step size of 0.002 ps at 300 K. Backbone N_i and O_{i+4} were restrained to a 2.8 Å distance, and backbone NH_i and O_{i+4} were restrained to a 1.8 Å distance in order to maintain the helical conformation. The centers of the helices were restrained to a distance of less than 10.5 Å over the entire length of the helices. Additional NOE-like restraints have been included to simulate the crosslinking results and the salt bridge: the CB distances of the crosslinked residues were restrained to be less than 5 Å. In case a Gly is involved in crosslinking, the CA-CB distance of the Gly and the crosslinking residue partner was restrained to be less than 6 Å. The salt bridge was included as a restraint of 2.5 Å between HE or HH1 of R995 and OD1 or OD2 of D723. The resulting structures were grouped into clusters. A cluster was defined as having at least ten structures with a relative rmsd of the backbone atoms of not more than 1.0 Å from one member of the cluster to at least one other member. Averaging all coordinates in a cluster and applying the same SA/MD scheme described above with this averaged structure as the starting conformation generated a representative structure of each cluster.

Two different helix lengths were calculated. Initially, only the TM domains including residues W967–V984 of αIIb and L694–A711 of β3 were used. In a second run, the helices were prolonged to include parts of the cytoplasmic domains. The longer helices entailed W967–R997 of αIIb and L694–F727 of β3.

Acknowledgments

I want to thank Andrei Lupas for help with the analysis of the coiled-coil structure, Mark Yeager for sending me his electron densities of integrins, Bill DeGrado for showing me his results prior to publishing, Tal Peleg-Shulman for critically reading the manuscript, and Horst Kessler for many stimulating discussions. The work was financed by the Minerva Foundation.

Received: January 10, 2005
Revised: February 3, 2005
Accepted: February 8, 2005
Published: May 10, 2005

References

Adair, B.D., and Yeager, M. (2002). Three-dimensional model of the human platelet integrin alpha IIbbeta 3 based on electron cryomicroscopy and X-ray crystallography. Proc. Natl. Acad. Sci. USA *99*, 14059–14064.

Adams, P.D., Arkin, I.T., Engelman, D.M., and Brunger, A.T. (1995). Computational searching and mutagenesis suggest a structure for the pentameric transmembrane domain of phospholamban. Nat. Struct. Biol. *2*, 154–162.

Adams, P.D., Engelman, D.M., and Brunger, A.T. (1996). Improved prediction for the structure of the dimeric transmembrane domain of glycophorin A obtained through global searching. Proteins *26*, 257–261.

Adams, P.D., Lee, A.S., Brunger, A.T., and Engelman, D.M. (1998). Models for the transmembrane region of the phospholamban pentamer: which is correct? Ann. N Y Acad. Sci. *853*, 178–185.

Armulik, A., Nilsson, I., von Heijne, G., and Johansson, S. (1999).

Determination of the border between the transmembrane and cytoplasmic domains of human integrin subunits. J. Biol. Chem. *274*, 37030–37034.

Brunger, A.T., Adams, P.D., Clore, G.M., DeLano, W.L., Gros, P., Grosse-Kunstleve, R.W., Jiang, J.S., Kuszewski, J., Nilges, M., Pannu, N.S., et al. (1998). Crystallography & NMR system: a new software suite for macromolecular structure determination. Acta Crystallogr. D Biol. Crystallogr. *54*, 905–921.

Bullough, P.A., Hughson, F.M., Skehel, J.J., and Wiley, D.C. (1994). Structure of influenza haemagglutinin at the pH of membrane fusion. Nature *371*, 37–43.

Crick, F.H. (1952). Is alpha-keratin a coiled coil? Nature *170*, 882–883.

Dehner, A., Planker, E., Gemmecker, G., Broxterman, Q.B., Bisson, W., Formaggio, F., Crisma, M., Toniolo, C., and Kessler, H. (2001). Solution structure, dimerization, and dynamics of a lipophilic alpha/3(10)-helical, C alpha-methylated peptide. Implications for folding of membrane proteins. J. Am. Chem. Soc. *123*, 6678–6686.

Dormitzer, P.R., Nason, E.B., Prasad, B.V., and Harrison, S.C. (2004). Structural rearrangements in the membrane penetration protein of a non-enveloped virus. Nature *430*, 1053–1058.

Fleming, K.G., and Engelman, D.M. (2001). Computation and mutagenesis suggest a right-handed structure for the synaptobrevin transmembrane dimer. Proteins *45*, 313–317.

Forrest, L.R., DeGrado, W.F., Dieckmann, G.R., and Sansom, M.S. (1998). Two models of the influenza A M2 channel domain: verification by comparison. Fold. Des. *3*, 443–448.

Gottschalk, K.E., and Kessler, H. (2004a). A computational model of transmembrane integrin clustering. Structure *12*, 1108–1115.

Gottschalk, K.E., and Kessler, H. (2004b). Evidence for hetero-association of transmembrane helices of integrins. FEBS Lett. *557*, 253–258.

Gottschalk, K.E., Adams, P.D., Brunger, A.T., and Kessler, H. (2002). Transmembrane signal transduction of the alpha(IIb)beta(3) integrin. Protein Sci. *11*, 1800–1812.

Gruber, M., and Lupas, A.N. (2003). Historical review: another 50th anniversary–new periodicities in coiled coils. Trends Biochem. Sci. *28*, 679–685.

Hughes, P.E., Diaz-Gonzalez, F., Leong, L., Wu, C., McDonald, J.A., Shattil, S.J., and Ginsberg, M.H. (1996). Breaking the integrin hinge. A defined structural constraint regulates integrin signaling. J. Biol. Chem. *271*, 6571–6574.

Humphries, M.J. (2000). Integrin structure. Biochem. Soc. Trans. *28*, 311–339.

Jorgensen, W.L., and Tiradorives, J. (1988). The Opls potential functions for proteins - energy minimizations for crystals of cyclic-peptides and crambin. J. Am. Chem. Soc. *110*, 1657–1666.

Kim, M., Carman, C.V., and Springer, T.A. (2003). Bidirectional transmembrane signaling by cytoplasmic domain separation in integrins. Science *301*, 1720–1725.

Kumar, C.C. (2003). Integrin alpha v beta 3 as a therapeutic target for blocking tumor-induced angiogenesis. Curr. Drug Targets *4*, 123–131.

Li, R., Babu, C.R., Lear, J.D., Wand, A.J., Bennett, J.S., and DeGrado, W.F. (2001). Oligomerization of the integrin alphaIIbbeta3: roles of the transmembrane and cytoplasmic domains. Proc. Natl. Acad. Sci. USA *98*, 12462–12467.

Li, R., Babu, C.R., Valentine, K., Lear, J.D., Wand, A.J., Bennett, J.S., and DeGrado, W.F. (2002). Characterization of the monomeric form of the transmembrane and cytoplasmic domains of the integrin beta 3 subunit by NMR spectroscopy. Biochemistry *41*, 15618–15624.

Li, R., Mitra, N., Gratkowski, H., Vilaire, G., Litvinov, R., Nagasami, C., Weisel, J.W., Lear, J.D., DeGrado, W.F., and Bennett, J.S. (2003). Activation of integrin alphaIIbbeta3 by modulation of transmembrane helix associations. Science *300*, 795–798.

Li, R., Bennett, J.S., and Degrado, W.F. (2004a). Structural basis for integrin alphaIIbbeta3 clustering. Biochem. Soc. Trans. *32*, 412–415.

Li, R., Gorelik, R., Nanda, V., Law, P.B., Lear, J.D., DeGrado, W.F., and Bennett, J.S. (2004b). Dimerization of the transmembrane domain of integrin {alpha}IIb subunit in cell membranes. J. Biol. Chem. *279*, 26666–26673.

Li, W., Metcalf, D., Gorelik, R., Li, R., Mitra, N., Nanda, V., Law, P.B., Lear, J.D., DeGrado, W.F., and Bennett, J.S. (2005). A push-pull mechanism for regulating integrin function. Proc. Natl. Acad. Sci. USA *102*, 1424–1429.

Lu, C., Takagi, J., and Springer, T.A. (2001). Association of the membrane proximal regions of the alpha and beta subunit cytoplasmic domains constrains an integrin in the inactive state. J. Biol. Chem. *276*, 14642–14648.

Luo, B.H., Springer, T.A., and Takagi, J. (2004). A specific interface between integrin transmembrane helices and affinity for ligand. PLoS Biol. *2*, E153.

Lupas, A.N., and Gruber, M. (2005). The structure of alpha-helical coiled coils. Adv. Protein Chem. *70*, 37–78.

Martin, K.H., Slack, J.K., Boerner, S.A., Martin, C.C., and Parsons, J.T. (2002). Integrin connections map: to infinity and beyond. Science *296*, 1652–1653.

Martin, J., Gruber, M., and Lupas, A.N. (2004). Coiled coils meet the chaperone world. Trends Biochem. Sci. *29*, 455–458.

Nooren, I.M., Kaptein, R., Sauer, R.T., and Boelens, R. (1999). The tetramerization domain of the Mnt repressor consists of two right-handed coiled coils. Nat. Struct. Biol. *6*, 755–759.

O'Shea, E.K., Klemm, J.D., Kim, P.S., and Alber, T. (1991). X-ray structure of the GCN4 leucine zipper, a two-stranded, parallel coiled coil. Science *254*, 539–544.

Pauling, L., and Corey, R.B. (1953). Compound helical configurations of polypeptide chains: structure of proteins of the alpha-keratin type. Nature *171*, 59–61.

Pauling, L., Corey, R.B., and Branson, H.R. (1951). The structure of proteins; two hydrogen-bonded helical configurations of the polypeptide chain. Proc. Natl. Acad. Sci. USA *37*, 205–211.

Sansom, M.S., Kerr, I.D., Smith, G.R., and Son, H.S. (1997). The influenza A virus M2 channel: a molecular modeling and simulation study. Virology *233*, 163–173.

Schneider, D., and Engelman, D.M. (2004). Involvement of transmembrane domain interactions in signal transduction by alpha/beta integrins. J. Biol. Chem. *279*, 9840–9846.

Stefansson, A., Armulik, A., Nilsson, I., von Heijne, G., and Johansson, S. (2004). Determination of N- and C-terminal borders of the transmembrane domain of integrin subunits. J. Biol. Chem. *279*, 21200–21205.

Stetefeld, J., Jenny, M., Schulthess, T., Landwehr, R., Engel, J., and Kammerer, R.A. (2000). Crystal structure of a naturally occurring parallel right-handed coiled coil tetramer. Nat. Struct. Biol. *7*, 772–776.

Takagi, J., Erickson, H.P., and Springer, T.A. (2001). C-terminal opening mimics 'inside-out' activation of integrin alpha5beta1. Nat. Struct. Biol. *8*, 412–416.

Takagi, J., Strokovich, K., Springer, T.A., and Walz, T. (2003). Structure of integrin alpha5beta1 in complex with fibronectin. EMBO J. *22*, 4607–4615.

Vinogradova, O., Haas, T., Plow, E.F., and Qin, J. (2000). A structural basis for integrin activation by the cytoplasmic tail of the alpha IIb-subunit. Proc. Natl. Acad. Sci. USA *97*, 1450–1455.

Vinogradova, O., Velyvis, A., Velyviene, A., Hu, B., Haas, T., Plow, E., and Qin, J. (2002). A structural mechanism of integrin alpha(IIb)-beta(3) "inside-out" activation as regulated by its cytoplasmic face. Cell *110*, 587–597.

Vinogradova, O., Vaynberg, J., Kong, X., Haas, T.A., Plow, E.F., and Qin, J. (2004). Membrane-mediated structural transitions at the cytoplasmic face during integrin activation. Proc. Natl. Acad. Sci. USA *101*, 4094–4099.

Weis, W.I., Brunger, A.T., Skehel, J.J., and Wiley, D.C. (1990). Refinement of the influenza virus hemagglutinin by simulated annealing. J. Mol. Biol. *212*, 737–761.

Weljie, A.M., Hwang, P.M., and Vogel, H.J. (2002). Solution struc-

tures of the cytoplasmic tail complex from platelet integrin alpha IIb- and beta 3-subunits. Proc. Natl. Acad. Sci. USA *99*, 5878–5883.

Xiao, T., Takagi, J., Coller, B.S., Wang, J.H., and Springer, T.A. (2004). Structural basis for allostery in integrins and binding to fibrinogen-mimetic therapeutics. Nature *432*, 59–67.

Xiong, J.P., Stehle, T., Diefenbach, B., Zhang, R., Dunker, R., Scott, D.L., Joachimiak, A., Goodman, S.L., and Arnaout, M.A. (2001). Crystal structure of the extracellular segment of integrin alpha Vbeta3. Science *294*, 339–345.

Xiong, J.P., Stehle, T., Zhang, R., Joachimiak, A., Frech, M., Goodman, S.L., and Arnaout, M.A. (2002). Crystal structure of the extracellular segment of integrin alpha Vbeta3 in complex with an Arg-Gly-Asp ligand. Science *296*, 151–155.